Static And Dynamic Characteristics of Double-Mode Inverter Under The Control of Single Current Loop

Jian Chu
Tianjin University of Technology and Education
Tianjin, 300222, China
wdjk2546@163.com

ABSTRACT: *This study aimed to explore static and dynamic characteristics of double-mode inverter under the control of single current loop. A model was established based on LC filter using grid-connected operation. With output power controlled by single current loop control method, key control parameters were figured out. Based on the simulation model established under Matlab/Simulink environment, favorable static and dynamic characteristics of double-mode inverter controlled by single current loop were verified.*

Keywords: Double- Mode Inverter, Grid- Connected Operation, Microgrid

Received: 1 October 2016, Revised 8 November 2016, Accepted 12 November 2016

1. Introduction

With the development and application of new energy, distributed power generation system will become the development direction of electric heating in the future [1]. A power electronic interface device called grid-connected inverter which can absorb or feedback energy to large power grid is generally equipped in distributed power generation system. Inverter in microgrid is applicable to grid-connected operation mode and independent operation mode, thus it is usually termed as double-mode inverter [2].

When power grid operates normally, inverter operating in grid-connected mode transfers redundant electric energy into power grid. When power grid fails, inverter will disconnect with power grid and operate in independent model to provide reliable electric energy [3,4]. Switching between two modes is usually smooth and rapid. Such a function similar to Uninterrupted Power Supply can effectively ensure reliable and safe operation of local load (UPS) [5,6]. Double-mode inverter plays a key role in the whole set of microgrid. How to improve the performance of double-mode inverter to meet the requirements of energy transmission, electric power quality and user diversity has become a hotspot of research.

Based on the analysis of single cycle control method, Jing Xiao from Shandong University realized digital single cycle control method, applied it into double-mode inverter operated under independent mode to highlight its advantages and made verification in MATLAC simulation environment [7]. To solve the problem of low respond speed of constant voltage control strategy of Z-source inverter, Harbin Institute of Technology designed grid-connection which can realize unity-power-factor grid connection and independent model of Z-source inverter which can ensure stable output voltage [8]. Based on closed-loop control system of single-phase inverter, Sun Xiangdong, Ren Biying, Zhang Qi et al. made analysis on the systematic performance of inverter under grid-connected mode, off-grid mode and smooth switching of modes [9]. To completely eliminate computation delay of active damping inner loop and grid-connected current outer loop, Aircraft Electric Power Source and Aerospace Technology Key Lab proposed double sampling model based real time computation method and moreover verified with experiment taking single phase LCL grid connected inverter as an example [10].

Based on the double-mode inverter operated under grid-connection mode, this study calculated key control parameters using single current loop control method, calculated key and established a simulation model under Matlab/Simulink environment to explore static and dynamic characteristics of double-mode inverter controlled by single current loop.

2. Selection of Filter of Double- Mode Inverter

In microgrid, there are mainly three kinds of commonly used filters for double-mode inverter, i.e., L filter, LC filter and LCL filter [11], as shown in figure 1. Three kinds of filters have their own features, thus we should make a choice based on the actual situation.

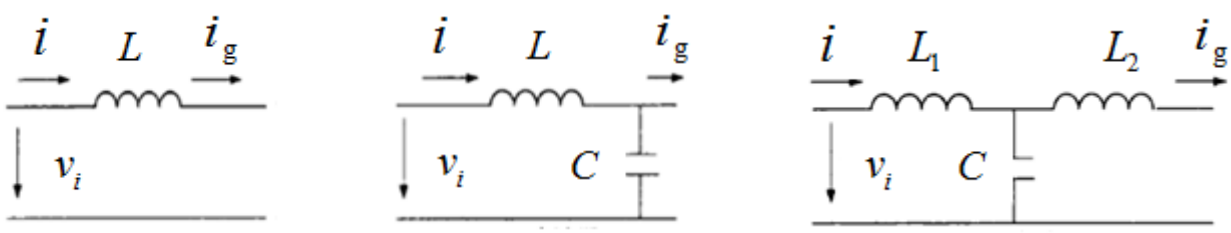

a. L filter b. LC filter c. LCL filter

Figure 1. Structure of common filters

Due to poor high frequency harmonic attenuation performance, L filter with simple structure requires higher inductance or lower switching frequency, in order to achieve ideal filter effect. Moreover, when double-mode inverter operating off grid controls output voltage, output voltage waveform is Pulse-Width Modulation (PWM) as single L filter cannot filter voltage; therefore, L filter suitable for grid-connection inverter with small power and high switching frequency is not applicable for double-mode inverter.

Compared to L filter, LCL filter is characterized by third order lowpass filtering. For the same harmonic standards and low switching frequency, LCL with relatively small filter inductance cam effectively reduce volume and loss. However, LCL filter also has defects. Due to the increase of capacitance branch, current control system turns from first order to third order, which make design of control system more difficult, and resonance limits wide application of LCL filter [12]. In formula (1), corresponding Bode diagram is shown in figure 2 if $L_1 = 2\times10^{-3}$H, $C = 12\times10^{-6}F$, $L_2 = 0.377\times10^{-3}$H. It indicates that, resonance generated by LCL filter within certain frequency can affect stability of the system.

$$\frac{I_g(s)}{V_i(s)} = \frac{1}{L_2CL_1s^3 + (L_1 + L_2)s} \tag{1}$$

For LCL filter such a third order system, detailed resonance can be figured out through formula (2). It is not hard to see that, three energy storage elements all have impact on resonant frequency.

$$\omega_{res} = \sqrt{\frac{L_1 + L_2}{L_1L_2C}} \tag{2}$$

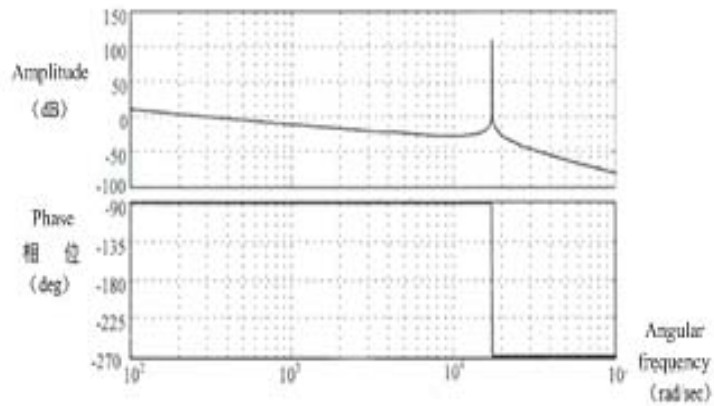

Figure 2. Bode diagram of LCL filter

LC filter has good filtering performance. When double-mode inverter operates in grid-connected mode, inductance can effectively filter grid-connected current. LC filter can not only effectively decay high frequency harmonic component in output voltage to obtain good waveform but also has advantages in cost [13]. Usually, double-mode inverter uses LC filter. This study also selects LC filter for research. When double-mode inverter operates under grid-connection mode, transmission characteristics with regard to output voltage and current is shown in formula (3).

$$\frac{I_g(s)}{V_i(s)} = \frac{1}{Ls} \tag{3}$$

The size of L is based on Total Harmonic Distortion (THD). Taking double-mode inverter with rated power of 25kVA, this study designed filter parameter that meets THD< 4%. When switching frequency is 6 kHz, direct current side voltage is 700 V and modulation degree is 0.768, harmonic voltage output by double-mode inverter under rated power is shown in figure 3.

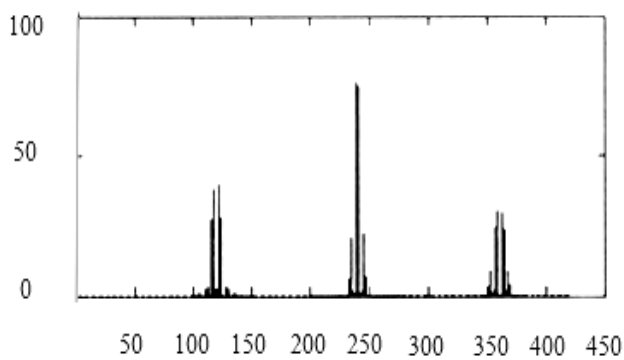

Figure 3. Harmonic voltage amplitude

Harmonic current computation formula is shown in formula (4). In the formula, ω_b is fundamental wave angular frequency and h=2, 3, 4 …

$$i(h) = \frac{u(h)}{L \times h \times \omega_b} \tag{4}$$

Computation formula for THD is shown in formula (5). In the formula, i_b is effective value of fundamental current, and at first, L is taken as 2 mH.

$$\mathrm{THD} = \frac{\sqrt{\sum_{h=2}^{420} i(h)^2}}{i_b} \times 100\% \tag{5}$$

When inverter is operated with rated power, $I_a = 38A$, THD = 3.15%; when it is operated with 80% rated power, $I_a = 30A$ and THD = 3.99%; when it is operated with 60% rated power, $I_a = 23A$, THD = 5.20%. With rated power, 2 mH of filter inductance can make THD< 4%.

3. Analysis of Doubleomode Inverter Opertaed Under Grid- Connected Mode

3.1 Mathematical model of double-mode inverter

When general mathematical model established for three-phase double-mode inverter, the assumption is as follows [14].

1) Voltage (e_a, e_b, e_c) is pure sinusoidal voltage with stable three phases.

2) Filter inductance L is linear, without considering saturation.

3) Switching loss resistance is reckoned in R, and the switch is perfect.

Firstly, logic switch function is defined as

$s_k (k = a、b、c)$.

$$S_k = \begin{cases} 1 \text{ (upper bridge arm breakover, lower bridge arm shutoff)} \\ 0 \text{ (upper bridge arm shutoff, lower bridge arm breakover)} \end{cases} \tag{6}$$

Kirchhoff Voltage Law is applied in a phase loop of double-mode inverter.

$$L\frac{di_a}{dt} + Ri_a = e_a - (v_{aN} + v_{NO}) \tag{7}$$

Under the condition of a-phase top tube breakover and down tube shutoff, $S_a = 1$ and $v_{aN} = V_{dc}$. Under the condition of a-phase top tube shutoff and down tube breakover, $S_a = 0$ and $v_{aN} = 0$. Formula (7) can be written into:

$$L\frac{di_a}{dt} + Ri_a = e_a - (v_{dc}s_a + v_{NO}) \tag{8}$$

Similarly, b-phase and c-phase voltage loop equation can be obtained, as follows:

$$L\frac{di_b}{dt} + Ri_b = e_b - (v_{dc}s_b + v_{NO}) \tag{9}$$

$$L\frac{di_c}{dt} + Ri_c = e_c - (v_{dc}s_c + v_{NO}) \tag{10}$$

Considering the research object is a three-phase balanced system, we have:

$$\sum_{k=a,b,c} e_k = \sum_{k=a,b,c} i_k = 0 \tag{11}$$

Combining (2-8) ~ (2-11), we get:

$$v_{NO} = -\frac{v_{dc}}{3}\sum_{k=a,b,c} s_k \tag{12}$$

Moreover, at any time point, double-mode inverter always has three conductive switching tunes, and there are totally eight switching modes. Therefore, direct current side current i_{dc} can be confirmed by the following formula:

$$i_{dc} = \sum_{k=a,b,c} i_k S_k \tag{13}$$

Kirchhoff ' s Current Law is used into direct current side capacitance, we get:

$$C\frac{dv_{dc}}{dt} = i_{dc} - i_L \tag{14}$$

Substitute formula (12) into formula (8) to (10) and (13) into (14), we get a mathematical model described by switching function in three-phase static coordinate by putting the above two formulas together.

$$\begin{cases} \mathrm{L}\frac{di_a}{dt} + Ri_a = e_a - v_{dc}(s_a - \frac{1}{3}\sum_{k=a,b,c} s_k) \\ \mathrm{L}\frac{di_b}{dt} + Ri_b = e_b - v_{dc}(s_b - \frac{1}{3}\sum_{k=a,b,c} s_k) \\ \mathrm{L}\frac{di_c}{dt} + Ri_c = e_c - v_{dc}(s_c - \frac{1}{3}\sum_{k=a,b,c} s_k) \\ C\frac{dv_{dc}}{dt} = \sum_{k=a,b,c} i_k s_k - i_L \end{cases} \tag{15}$$

Suppose voltage of double-mode inverter on alternating current side is u_a , u_b and u_c respectively. According to the mathematical model described by formula (15), we get:

$$\begin{cases} u_a = v_{dc}(s_a - \frac{1}{3}\sum_{k=a,b,c} s_k) \\ u_b = v_{dc}(s_b - \frac{1}{3}\sum_{k=a,b,c} s_k) \\ u_c = v_{dc}(s_c - \frac{1}{3}\sum_{k=a,b,c} s_k) \end{cases} \tag{16}$$

Such mathematical model for double-mode inverter in three-phase static coordinate contains alternating quantity, which is not beneficial to design of control system. Thus we can transform three-phase static coordinate into rotating coordinate system which synchronously rotates with fundamental frequency [15]. After transformation, all alternating quantities which have the same frequency with fundamental wave of power system are turned into direct current quantity, which can simplify design of control system. Coordinate transformation can be divided into two categories, i.e., equal quantity conversion and equal power conversion. Difference of them lies on whether transformational matrix is orthorhombic or not. This study uses equal quantity coordinate conversion.

In figure 4, there is an 120° between a axis, b axis and c axis; β axis and α axis is perpendicular; α axis and a axis is coincident and there is an 90° angle between a axis (α axis) and β axis; angle between a axis and d axis is ωt. It can be deduced that, vector x transforming from three-phase static coordinate (abc) into two-phase rotational coordinate meets the formula

$$\begin{bmatrix} v_d \\ v_q \end{bmatrix} = \begin{bmatrix} \cos\theta & \sin\theta \\ -\sin\theta & \cos\theta \end{bmatrix} \bullet \begin{bmatrix} 1 & 0 \\ \frac{1}{\sqrt{3}} & \frac{2}{\sqrt{3}} \end{bmatrix} \begin{bmatrix} v_a \\ v_b \end{bmatrix} \tag{17}$$

Substituting formula (17) into formula (15), we get a mathematical model of three-phase double-mode inverter in two-phase rotational coordinate:

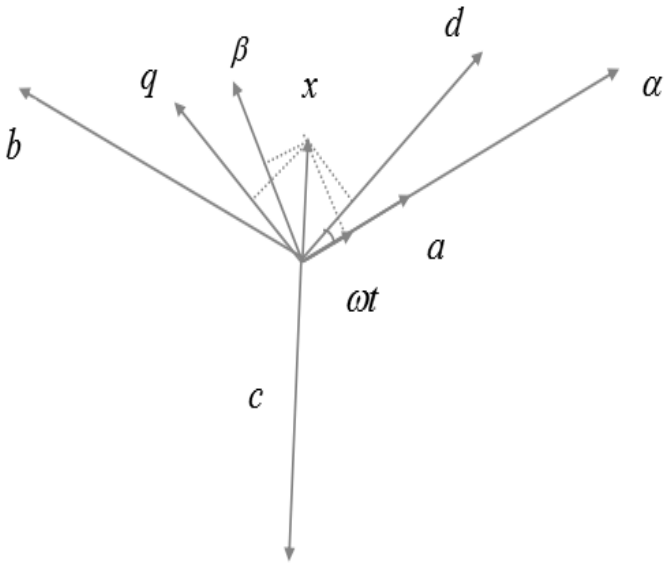

Figure 4. Coordinate and vector decomposition

$$\begin{cases} L\dfrac{di_d}{dt} = -Ri_d + \omega Li_q + e_d - u_d \\ L\dfrac{di_q}{dt} = -Ri_q + \omega Li_d + e_q - u_q \\ C\dfrac{dv_{dc}}{dt} = \dfrac{3}{2}(s_d i_d + s_q i_q) - i_L \end{cases} \tag{18}$$

In formula, u_k, i_k, e_k (k=d, q) is output voltage, current and voltage component in d axis and q axis, respectively. Detailed deduction process of mathematical model for three-phase double-mode inverter is given above, and finally a mathematical model of the inverter in two-phase synchronous rotating reference frame is obtained. Fundamental components of electric quantity in dq coordinate are all direct current quantity, which simplifies design of control system. On the other hand, network voltage vector is usually taken as the reference vector of dq rotational coordinate, i.e., d axis and network voltage vector is coincident. Under such condition, d axis becomes active reference axis and q axis becomes reactive reference axis. Decoupled active power and reactive power can be controlled separately.

4. Design of Regulator

Mature directed vector control based on network voltage is taken as the control strategy of double-mode inverter operated with grid-connected mode in this study [16]. Voltage-oriented control is composed of outer loop of direct voltage, active current inter-loop and reactive current inter-loop. The function of outer-loop of direct voltage is to stabilize direct voltage, thus voltage loop can be ignored and the control system can be simplified into single current loop control if double-mode inverter is unnecessary for stabilize or regulate direct current side voltage. Moreover, design of current loop determines whether the whole control system can ensure high-performance steady-state operation and fast dynamic response to a large extent.

In this study, grid-connected mode of double mode inverter is controlled by single loop based on bridge inductive current. As to the design of controller with dq synchronous rotating reference frame, we should first make laplace transformation on current equation of double-mode inverter in synchronous rotating reference frame [17] and ignore equivalent resistance R.

$$\begin{cases} (\mathrm{R} + Ls)\ I_d(s) = \omega LI_q + E_d(s) - U_d(s) \\ (\mathrm{R} + Ls)\ I_q(s) = \omega LI_d + E_q(s) - U_q(s) \end{cases} \tag{19}$$

Thus control system of major loop is obtained, as shown in figure 5.

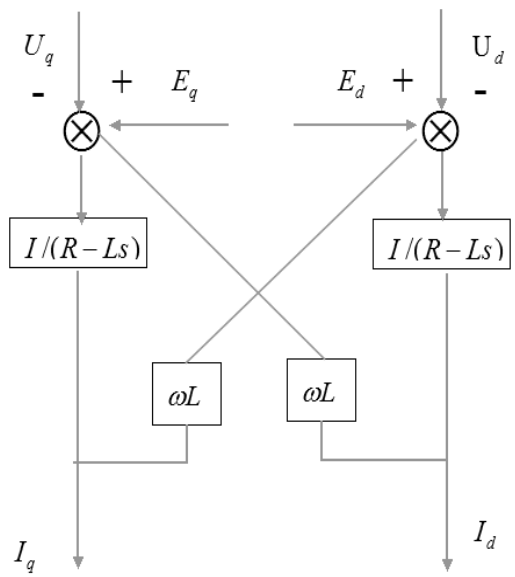

Figure 5. Major loop control graph

It can be seen from figure 5 that, current in d axis and q axis is coupled in the control system. Usually, feedforward decoupling is used for designing controller. When current regulator is controlled by proportional integral (PI), control equation for u_d and u_q is as follows:

$$u_d = -(K_{ip} + \frac{K_{iI}}{s})(i_d^* - i_d) + \omega L i_q + e_d \tag{20}$$

$$u_q = -(K_{ip} + \frac{K_{iI}}{s})(i_q^* - i_q) + \omega L i_d \tag{21}$$

From formula (20) and (21), we get PI control diagram of double-mode inverter in dq coordinate (Table 6).

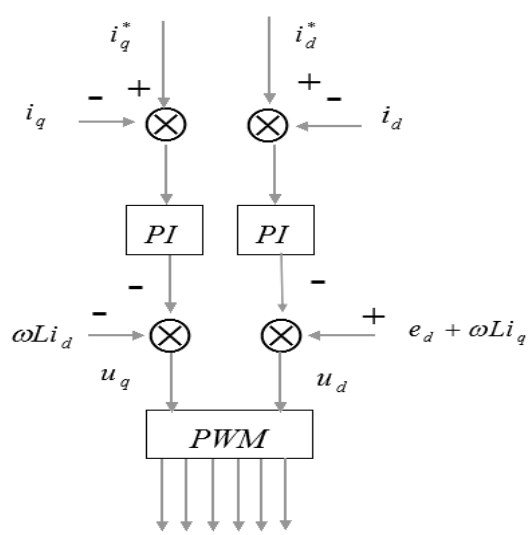

Figure 6. PI control diagram of double-mode inverter in dq coordinate

In figure 7, K_{ip} and K_{iI} is proportional coefficient and integral coefficient. Substitute formula (20) and (21) into formula (19). Considering delay of current loop signal sampling and low inertia of PWM control and ignoring intervention of network voltage, we can get current loop control structure. d axis is taken as an example.

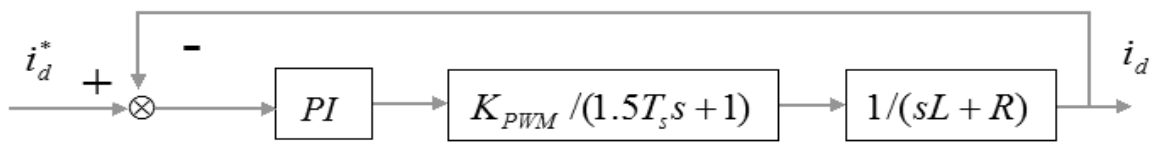

Figure 7. Current loop control structure

Its closed loop transfer function is:

$$G_i(s) = \frac{(sK_{ip} + K_{iI})}{s^2 L + (R + K_{ip})s + K_{iI}} \tag{22}$$

Parameters of current loop can be designed according to typical type I or II system. The former can make current have good tracking performance; but once network voltage is interfered, it is hard to recover. Though overshoot is large during tracking current step command with type II system, current loop can recover quickly from intervention. This study selects typical type II system and sets K_{ip} = 4.8 and K_{iI} = 3840. Referring to practical parameters, we suppose L=2 mH and R=0.06 Ω. Next, we get amplitude-frequency and phase-frequency response curve of transfer function. As shown in figure 8, bandwidth of current inter loop is wide and response is quite fast.

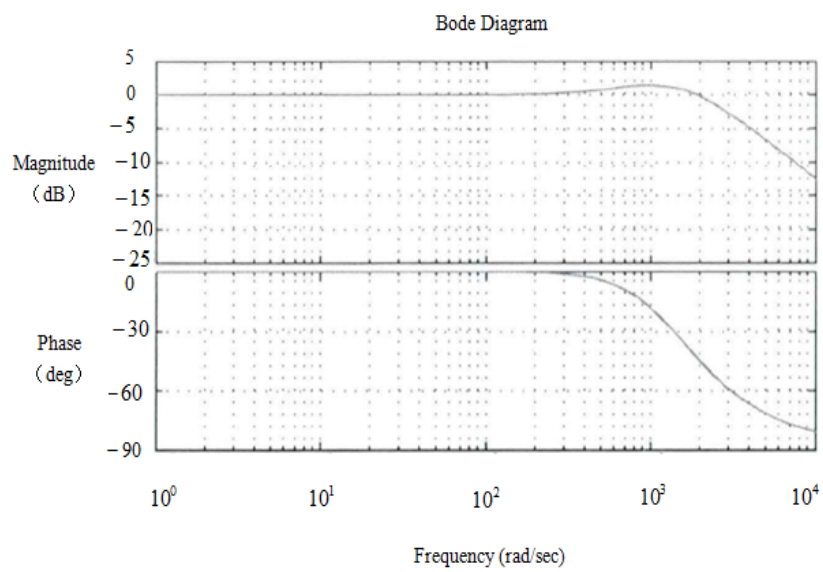

Figure 8. Magnitude versus phase plot of close loop of grid-connection controller

5. Grid-Connected Operation Simulation

To verify the effectiveness of controller designed above and compare PI parameters designed with typical type I or II system, we establish a simulation model in Matlab/Simulink. Detailed hardware parameters are shown in table 1.

In the simulation model, direct current side is parallelly connected with 700V direct current and alternating current side is connected with direct current with 380V. Reactive current is set as 0 and active current is set as 10A at first. At

Parameter	Value
Filter capacitor C_f	$12\mu F$
Filter inductance L	$2mH$
Equivalent resistance R	0.06Ω
Switching frequency f_s	$6KHz$

Table 1. simulation parameter of hardware of double-mode inverter

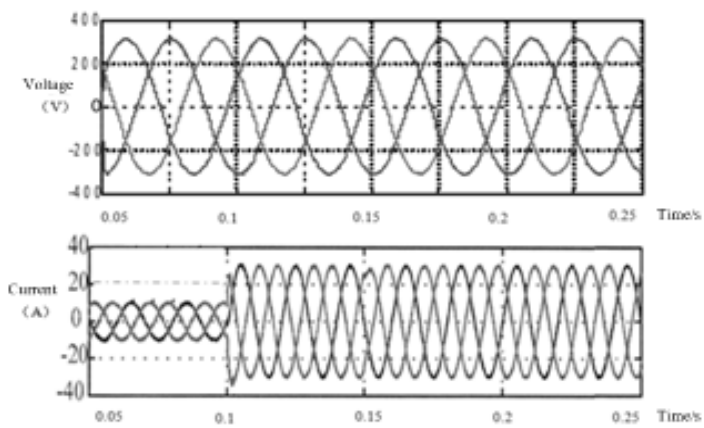

Figure 9. Arc voltage and current waveforms under grid-connection mode

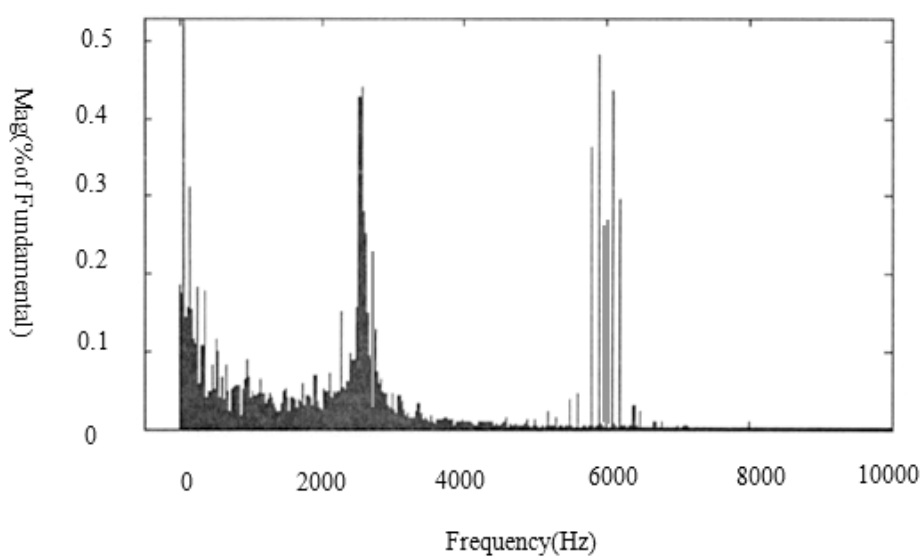

Figure 10. FFT analysis of output current of double-mode inverter

0.1 s, the set value turns to be 30 A and at 0.15 s, 30 V^{ed} interventions occur. PI parameter KiP and KiI designed by typical type I system is 4 and 120 respectively, and parameters designed by typical type II system is 4.8 and 3840 respectively. Simulation waveform is shown in figure 9 and 10.

Figure 11 is comparison of step response of current i_d when current regular is designed in two different ways.

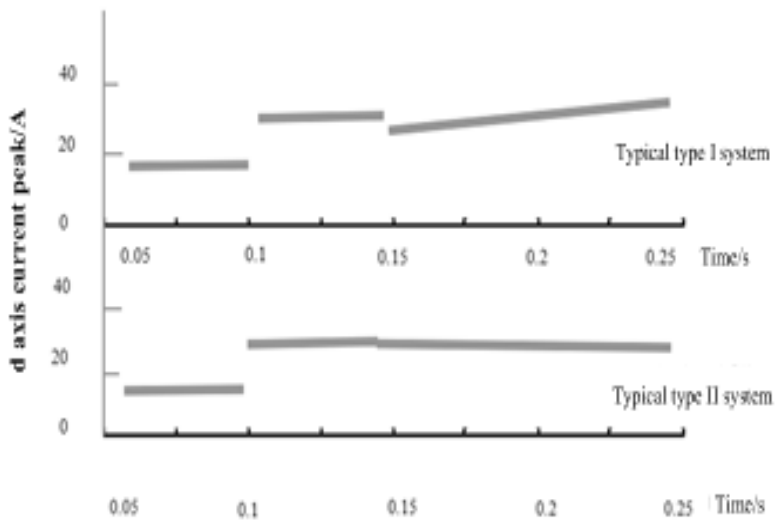

Figure 10. Comparison of step response of current i_d

6. Conclusion

It can be seen from figure 9 and 10, when single current loop controlled double-mode inverter operates in grid-connection mode, it can output current with good quality; when current order changes suddenly, the inverter can rapidly track output current order and shows up favorable static and dynamic characteristics.

It can be seen from figure 11 that, when current regulator is designed according to typical type 1 system, current i_d shows good tracing performance; but once e_d disturbance occurs, recovery time of i_d is long; however, when current regulator is designed according to typical type 2 system, current loop can recover rapidly under the disturbance of e_d.

Conflict of Interest

The author(s) confirm that this article content has no conflicts of interest.

References

[1] Shuang, Y. (2014). Development Pattern of Distributed Energy Resource in the Environment of Intelligent Power Grid. *Science and Technology,* (24) 42-42.

[2] Lingemann, M., Ortjohann, E., Schmelter, A. (2010). Inverters as Smart Grid Interface - Standardized Feeding Modes for Different Distributed Generation Units and Grid Requirements, *Power Electronics,* (4) 14-19.

[3] Xucheng, L., Pin, Y., Yin, L. (2011). Research of Dual Modes Inverter Based on DSP, *Power Electronics,* 45 (2) 56-59.

[4] Debin, Z., Fang, L., Haizhen, X., Xing, Z. (2012). Control Strategy for Distributed Generation Inverter in Two Modes Operation of Microgrid. *Power Electronics,* 46 (10) 9-10.

[5] Hui, X. (2014). Analysis of UPS with Non-output Transformer. *Components and Powder,* (4) 134-141.

[6] Jianjun, J. (2013). Working Principle of UPS and its Application in Instruments in Computer Room. *Technological Development of Enterprise,* (4) 20-21.

[7] Guangxian, Z. (2014). Design and Implementation of Double-pattern Inverter. Shandong University.

[8] Qian, Y., Huihui, D., Yanbin, Q. (2014). Research on Control Strategy of Z-Source Inverter with Double Mode of Grid-Connection and Stand-Alone. *Electrical Measurement & Instrumentation*, 51 (6) 55-59.

[9] Xiangdong, S., Biying, R., Qi, Z., Gang, L. (2014). Grid-connected and Off-grid Modes for a Single-phase Micro-grid Inverter. *Power Electronics*, 48 (1) 1-3.

[10] Donsheng, Y., Xinbo, R., Heng, W. (2015). A Real-time Computation Method with Dual Sampling Modes to Improve the Current Control Performance of the LCL-type Grid-connected Inverter. *Proceedings of the CSEE*, (6) 1445-1454.

[11] Zhiying, X. (2009). Current Control Technology of Grid-connected Inverter. Nanjing University of Aeronautics and Astronautics.

[12] Yingping, Y., Kaiping, L., Lin, W. (2011). Control Strategy of LCL-filter-based Inverter for Photovoltaic Grid Connection. *Electric Power Automation Equipment*, 31 (12) 54-58.

[13] Ji, J., Shanxu, D., Zhongwei, C. (2012). Research on Control Strategy for Three-Phase Double Mode Inverter. *Transactions of China Electrotechnical Society*, (2) 52-58.

[14] Xiaohuan, W., Chunjiang, Z., Feng, D. (2010). Design and Implementation of Three-phase Inverter Controller with Double Mode of Grid-connection and Stand-alone. *Power Electronics*, 44 (12) 82-84.

[15] Guiying, L., Shiping, S., Zhiqing, Q. (2010). A New Harmonic Detection Method for Three-phase Four-Wire System Based on Orthogonal Transformation of Multi-Frequency Rotating Coordinate. *Power System Technology*, 34 (7) 87-93.

[16] Yufeng, W., Linwei, Z., Tao, L., Guohua, L. (2014). Research on Three-phase VSI Cascade Photovoltaic Grid-connected Inverter. *Power Electronics*, 48(4) 55-57.

[17] Lianfu, W., Peiyan, F., Xiaohua, S. (2013). New Passive Lossless Snubber Circuit. *Chinese Journal of Power Sources*, 37(2) 285-288.